Excitons in two coupled conjugated polymer chains



1996 J. Phys.: Condens. Matter 8 8847

(http://iopscience.iop.org/0953-8984/8/45/018)

J. Phys.: Condens. Matter **8** (1996) 8847–8857. Printed in the UK

# Excitons in two coupled conjugated polymer chains

Z G Yu†‡, M W Wu§, X S Rao‡, X Sun‡ and A R Bishop†

† Theoretical Division, Los Alamos National Laboratory, Los Alamos, NM 87545, USA‖
‡ T D Lee Laboratory of Physics Department, Fudan University, Shanghai 200433, and National Laboratory of Infrared Physics, Shanghai 200083, People's Republic of China
§ Department of Physics and Engineering Physics, Stevens Institute of Technology, Hoboken, NJ 07030, USA

Received 21 May 1996

**Abstract.** We have studied the exciton states in two coupled conjugated polymer chains which are modelled individually by the Su–Schrieffer–Heeger Hamiltonian and coupled by an interchain electron-transfer term. Both the intra- and interchain long-range Coulomb interactions are taken into account. The properties of the lowest symmetric and anti-symmetric exciton states are extensively discussed for both the parallel and anti-parallel ordering between these two chains. It is found that, for these two kinds of ordering, the features of excitons are quite different. Possible implications for the experiment of luminescent polymers are also addressed.

## 1. Introduction

The significance of excitons in conjugated polymers in a class known as polydiacetylene has been recognized for many years [1]. Recently, the interest in excitons has been heightened by discovering that poly(*p*-phenylene vinylene) (PPV) and its derivatives can be used as the active luminescent layer in electroluminescent light-emitting diode devices [2], since it is believed that radiative recombination of singlet excitons gives rise to luminescence. Although a general picture and understanding of photoinduced absorption (PA) and photoconductivity (PC) experiments on PPV and its derivatives remains a subject of intense debate [3–11], the dramatically different PA behaviour of dilute solutions and thin films of poly[2-methoxy, 5-(2′ ethyl-hexoxy)-1, 4 phenylene vinylene] (MEH-PPV) [12], together with the photoconductivity being observed to start at the absorption edge in PPV [13], clearly indicate the important role that the interchain coupling plays. In fact, electron diffraction experiments indicate that the interchain coherence length of PPV is about 60 Å [14]. However, the properties of excitons in coupled chains have, to the best of our knowledge, never been discussed.

There have been several studies aimed at developing the exciton theory in a single-polymer chain [15–18]. Abe and co-workers introduced the standard exciton theory [19] to one-dimensional polymers [18]. Within the single-configuration-interaction (SCI) approximation, the energy levels and wave functions of exciton states in a long chain can be obtained. In this paper, we will extend the approach of Abe and co-workers and explore the features of excitons in two coupled polymer chains. Interestingly enough, we find that, for two kinds of ordering, i.e., parallel and anti-parallel ordering between the two chains, the properties of excitons are quite different. Although this study does not result

‖ Mailing address.

0953-8984/96/458847+11$19.50  

in quantitative explanations of the PA and PC experiments, it is helpful for understanding better the photophysics of luminescent polymers like PPV, and is also a foundation for further calculations of optical properties of coupled polymers.

In section 2, the model is defined and the formulation is derived. In section 3, we present numerical results on the lowest symmetric and anti-symmetric excitons and discuss some implications for experiments.

## 2. Formalism

We start with the two-coupled-chains model introduced by Baeriswyl and Maki [20], in which each chain is described by the Su–Schrieffer–Heeger Hamiltonian (SSH) [21]

$$H_j = -t \sum_n [1 - (-1)^n z_j](c^\dagger_{jn+1} c_{jn} + \text{HC}) \tag{1}$$

where $j = 1, 2$ denotes the chain index, and is coupled by an interchain hopping term

$$H_\perp = -t_\perp \sum_n (c^\dagger_{1n} c_{2n} + \text{HC}). \tag{2}$$

Here $c_{jn}$ is the annihilation operator of the electron at site $n$ on the $j$th chain, and the spin indices have been omitted for simplicity. Each chain is assumed to be dimerized in accordance with the Peierls theorem [22], $z_j$ is the dimerization amplitude of the $j$th chain, and $|z_1| = |z_2| = z$, but they may differ in sign. Strictly speaking, the SSH model is directly applicable only to polyacetylene; however, recent work has shown that the primary excitation in luminescent polymers like PPV can also be described within the linear chain model [23, 10, 11]. In PPV and its derivatives, the lowest excitonic wave function extends over several repeat units [9, 13]; the properties of excitons are therefore not very sensitive to the delicate structure within the unit. From the viewpoint of renormalization [24], we can map the complex structure of PPV into an effective SSH system with the same significant physical properties by integrating out the freedom of benzene rings and only considering the electrons on the nonbenzene carbon atoms [10]. Thus the features of the exciton in the SSH model must have some implications for that in luminescent polymers. We have also adopted the rigid-lattice approximation, since many experiments and theories have demonstrated that the primary excitation is the exciton, and electron–electron interactions are dominant over electron–lattice interactions in luminescent polymers [5, 7, 8, 10, 11, 23]. Theoretical studies that have taken into account the electron–lattice interaction also show that incorporation of the lattice relaxation effect would not lead to an increase in binding energy of the exciton [25]. This simplification enables us to handle electron–electron interactions in long chains and arrive at an understanding of *electronic states* in luminescent polymers without loss of essential physics, although the quantitative explanation of a *lattice* property like vibronic structure or bond length should, in fact, take into account the lattice relaxation effects [26].

By introducing operators $a_{jk}$ and $b_{jk}$ through the relation (we take the lattice constant $a = 1$ in this section) [20]

$$c_{jn} = \frac{1}{\sqrt{N}} \sum_k \mathrm{e}^{\mathrm{i}kn}[(-1)^n a_{jk} + \mathrm{i} b_{jk}] \tag{3}$$

where $N$ is the number of sites per chain, and by using the Bogoliubov transformation

$$\begin{pmatrix} a_{jk} \\ b_{jk} \end{pmatrix} = \begin{pmatrix} \cos\theta_{jk} & \sin\theta_{jk} \\ -\sin\theta_{jk} & \cos\theta_{jk} \end{pmatrix} \begin{pmatrix} \alpha_{jk} \\ \beta_{jk} \end{pmatrix} \tag{4}$$

$H_j$ is diagonalized when $\tan 2\theta_{jk} = z_j \tan k$:

$$H_j = \sum_k E_k(\alpha_{jk}^\dagger \alpha_{jk} - \beta_{jk}^\dagger \beta_{jk}) \tag{5}$$

with

$$E_k = 2t\sqrt{\cos^2 k + z_j^2 \sin^2 k}. \tag{6}$$

The interchain hopping term then becomes

$$H_\perp = -t_\perp \sum_k [\cos(\theta_{1k} - \theta_{2k})(\alpha_{1k}^\dagger \alpha_{2k} + \beta_{1k}^\dagger \beta_{2k}) + \sin(\theta_{1k} - \theta_{2k})(\beta_{1k}^\dagger \alpha_{2k} - \alpha_{1k}^\dagger \beta_{2k}) + \text{HC}]. \tag{7}$$

There are two kinds of ordering between the two chains: parallel ordering ($\theta_{1k} = \theta_{2k}$) and anti-parallel ordering ($\theta_{1k} = -\theta_{2k}$) [20]. For the case where $\theta_{1k} = \theta_{2k}$,

$$H_\perp = -t_\perp \sum_k (\alpha_{1k}^\dagger \alpha_{2k} + \beta_{1k}^\dagger \beta_{2k} + \text{HC}) \tag{8}$$

and the full Hamiltonian $H = H_1 + H_2 + H_\perp$ can be written as

$$H = \sum_k (\alpha_{1k}^\dagger \alpha_{2k}^\dagger) \begin{pmatrix} E_k & -t_\perp \\ -t_\perp & E_k \end{pmatrix} \begin{pmatrix} \alpha_{1k} \\ \alpha_{2k} \end{pmatrix} + \sum_k (\beta_{1k}^\dagger \beta_{2k}^\dagger) \begin{pmatrix} -E_k & -t_\perp \\ -t_\perp & -E_k \end{pmatrix} \begin{pmatrix} \beta_{1k} \\ \beta_{2k} \end{pmatrix} \tag{9}$$

and is readily diagonalized by the orthogonal transformation

$$(A_{1k}\ A_{2k}\ B_{1k}\ B_{2k})^{\mathrm{T}} = \mathbf{O}(\alpha_{1k}\ \alpha_{2k}\ \beta_{1k}\ \beta_{2k})^{\mathrm{T}} \tag{10}$$

$$H = \sum_k [(E_k - t_\perp)(A_{1k}^\dagger A_{1k} - B_{1k}^\dagger B_{1k}) + (E_k + t_\perp)(A_{2k}^\dagger A_{2k} - B_{2k}^\dagger B_{2k})] \tag{11}$$

where, $A_{ik}^\dagger$ and $B_{ik}^\dagger$ ($i = 1, 2$) create an electron in the $i$th conduction and valence bands respectively.

For the case where $\theta_{1k} = -\theta_{2k} = \theta_k$,

$$H_\perp = -t_\perp \sum_k [\cos 2\theta_k (\alpha_{1k}^\dagger \alpha_{2k} + \beta_{1k}^\dagger \beta_{2k}) + \sin 2\theta_k (\beta_{1k}^\dagger \alpha_{2k} - \alpha_{1k}^\dagger \beta_{2k}) + \text{HC}] \tag{12}$$

and the total Hamiltonian reads

$$H = \sum_k (\alpha_{1k}^\dagger\ \alpha_{2k}^\dagger\ \beta_{1k}^\dagger\ \beta_{2k}^\dagger) \times \begin{pmatrix} E_k & -t_\perp \cos 2\theta_k & 0 & t_\perp \sin 2\theta_k \\ -t_\perp \cos 2\theta_k & E_k & -t_\perp \sin 2\theta_k & 0 \\ 0 & -t_\perp \sin 2\theta_k & -E_k & -t_\perp \cos 2\theta_k \\ t_\perp \sin 2\theta_k & 0 & -t_\perp \cos 2\theta_k & -E_k \end{pmatrix} \begin{pmatrix} \alpha_{1k} \\ \alpha_{2k} \\ \beta_{1k} \\ \beta_{2k} \end{pmatrix}. \tag{13}$$

Making the orthogonal transformation $\mathbf{O}$, we obtain the diagonalized Hamiltonian

$$H = \sum_k [\varepsilon_{1k}(A_{1k}^\dagger A_{1k} - B_{1k}^\dagger B_{1k}) + \varepsilon_{2k}(A_{2k}^\dagger A_{2k} - B_{2k}^\dagger B_{2k})] \tag{14}$$

with

$$\varepsilon_{1k} = \sqrt{E_k^2 + t_\perp^2 + 4tt_\perp \cos k} \tag{15}$$

$$\varepsilon_{2k} = \sqrt{E_k^2 + t_\perp^2 - 4tt_\perp \cos k} \tag{16}$$

and, at the same time, the transformation matrix $\mathbf{O}$.

We add the long-range Coulomb interaction $H_{e-e}$ to $H$ and study the exciton state:

$$H_{e-e} = \frac{1}{2}\sum_{IJll'}\sum_{ss'} V_{ll'}^{IJ}\rho_{Ils}\rho_{Jl's'} \tag{17}$$

where $\rho_{Ils} = c_{Ils}^{\dagger}c_{Ils} - 1/2$, $I$ and $J$ are the chain indices, and the interaction potential

$$V_{ll'}^{IJ} = \begin{cases} V_{ll'} & I = J \\ \tilde{V}_{ll'} & I \neq J. \end{cases}$$

The intrachain Coulomb interaction is the commonly used form [18]

$$V_{ll} = U$$
$$V_{ll'} = \frac{V}{|l-l'|} \qquad (l \neq l').$$

Here $U$ is the on-site Hubbard repulsion, and $V$ the nearest-neighbour Coulomb interaction. We assume that the interaction potential between the two chains has a relatively simple form:

$$\tilde{V}_{ll'} = \frac{\tilde{U}}{\sqrt{R_0^2 + (l-l')^2}}.$$

$R_0$ will be set to 1 in following calculations.

The procedure to determine the exciton state is a standard one. First, we use the single-particle state of $H$ to construct the ground state $|g\rangle$:

$$|g\rangle = \prod_{jk} B_{jk\uparrow}^{\dagger}B_{jk\downarrow}^{\dagger}|0\rangle.$$

Within the SCI approximation, the exciton state can be achieved by diagonalizing the Hamiltonian $H + H_{e-e}$ in the subspace of the single electron–hole excitation:

$$|i, k_c; j, k_v\rangle \equiv \frac{1}{\sqrt{2}}(A_{ik_c\uparrow}^{\dagger}B_{jk_v\uparrow} \pm A_{ik_c\downarrow}^{\dagger}B_{jk_v\downarrow})|g\rangle \tag{18}$$

where $+$ is for the spin singlet, and $-$ for one of the triplet. $k_c$ and $-k_v$ are momenta of the electron in the conduction band and the hole in the valence band, respectively. $i$ and $j$ $(=1, 2)$ are the band indices.

For the spin-singlet exciton,

$$\begin{aligned}\langle i', k_c'; j', k_v'|H + H_{e-e} - E_0|i, k_c; j, k_v\rangle &= \delta_{k_v', k_v}\delta_{k_c', k_c}\left[\delta_{jj'}\left(\delta_{ii'}\varepsilon_{ik_c} + \sum_{IJll'} V_{ll'}^{IJ}\langle A_{i'k_c}c_{Jl'}^{\dagger}\rangle\langle c_{Jl'}c_{Il}^{\dagger}\rangle\langle c_{Il}A_{ik_c}^{\dagger}\rangle\right)\right. \\ &\left. + \delta_{ii'}\left(-\delta_{jj'}\varepsilon_{jk_v} - \sum_{IJll'} V_{ll'}^{IJ}\langle B_{j'k_v}^{\dagger}c_{Jl'}\rangle\langle c_{Il}c_{Jl'}^{\dagger}\rangle\langle c_{Il}^{\dagger}B_{jk_v}\rangle\right)\right] + 2E_X - E_C \end{aligned} \tag{19}$$

where $E_0 = \langle g|H + H_{e-e}|g\rangle$, and for the triplet,

$$\begin{aligned}\langle i', k_c'; j', k_v'|H + H_{e-e} - E_0|i, k_c; j, k_v\rangle &= \delta_{k_v', k_v}\delta_{k_c', k_c}\left[\delta_{jj'}\left(\delta_{ii'}\varepsilon_{ik_c} + \sum_{IJll'} V_{ll'}^{IJ}\langle A_{i'k_c}c_{Jl'}^{\dagger}\rangle\langle c_{Jl'}c_{Il}^{\dagger}\rangle\langle c_{Il}A_{ik_c}^{\dagger}\rangle\right)\right. \\ &\left. + \delta_{ii'}\left(-\delta_{jj'}\varepsilon_{jk_v} - \sum_{IJll'} V_{ll'}^{IJ}\langle B_{j'k_v}^{\dagger}c_{Jl'}\rangle\langle c_{Il}c_{Jl'}^{\dagger}\rangle\langle c_{Il}^{\dagger}B_{jk_v}\rangle\right)\right] - E_C \end{aligned} \tag{20}$$

and

$$E_X = \sum_{IJll'} V_{ll'}^{IJ} \langle A_{i'k_c'} c_{Il}^\dagger \rangle \langle c_{Jl'} A_{ik_c}^\dagger \rangle \langle B_{j'k_v'}^\dagger c_{Il} \rangle \langle c_{Jl'}^\dagger B_{jk_v} \rangle \tag{21}$$

$$E_C = \sum_{IJll'} V_{ll'}^{IJ} \langle A_{i'k_c'} c_{Jl'}^\dagger \rangle \langle c_{Jl'} A_{ik_c}^\dagger \rangle \langle B_{j'k_v'}^\dagger c_{Il} \rangle \langle c_{Il}^\dagger B_{jk_v} \rangle \tag{22}$$

where $\langle \cdots \rangle \equiv \langle g| \cdots |g \rangle$. We show how to evaluate $\langle c_{Il}^\dagger A_{ik_c} \rangle$, $\langle B_{jk_v}^\dagger c_{Il} \rangle$, and $\langle c_{Jl'}^\dagger c_{Il} \rangle$ in the appendix.

This two-coupled-chain system also has symmetry with respect to the spatial inversion at a bond centre like a single chain. The inversion operator $R$ is defined by

$$R[c_{jn}] = c_{jN-n+1} \tag{23}$$

and it is easy to prove that

$$R[\alpha_{jk}^\dagger] = -\mathrm{e}^{\mathrm{i}k} \alpha_{j-k}^\dagger \qquad R[\beta_{jk}] = \mathrm{e}^{-\mathrm{i}k} \beta_{j-k}$$

and so

$$\alpha_{ik_c}^\dagger \beta_{jk_v} |g\rangle \xrightarrow{R} -\mathrm{e}^{\mathrm{i}(k_c - k_v)} \alpha_{-ik_c}^\dagger \beta_{j-k_v} |g\rangle \tag{24}$$

and from the transformation matrix **O**, which diagonalizes the Hamiltonians (9) and (13), we also have

$$|i, k_c; j, k_v\rangle \xrightarrow{R} -\mathrm{e}^{\mathrm{i}(k_c - k_v)} |i, -k_c; j, -k_v\rangle. \tag{25}$$

Thus we can construct the symmetric state ($A$) and the anti-symmetric one ($B$). The $A$-state is written as

$$|i, k_c; j, k_v; -\rangle = \frac{1}{\sqrt{2}} (|i, k_c; j, k_v\rangle - \mathrm{e}^{\mathrm{i}(k_c - k_v)} |i, -k_c; j, -k_v\rangle) \tag{26}$$

and the $B$-state is

$$|i, k_c; j, k_v; +\rangle = \frac{1}{\sqrt{2}} (|i, k_c; j, k_v\rangle + \mathrm{e}^{\mathrm{i}(k_c - k_v)} |i, -k_c; j, -k_v\rangle). \tag{27}$$

In the numerical calculation, we may confine ourselves to the $A$- or $B$-subspaces to diagonalize the Hamiltonian $H + H_{e-e}$ since the matrix element connecting $A$- and $B$-states vanish. In the exciton state, the relative motion and centre-of-mass motion can also be separated by introducing the variables $k$ and $K$ so that $k_c = k + K$ and $k_v = k - K$. $k$ and $2K$ are the momenta of the relative motion and centre-of-mass motion of the electron–hole pair. Since we are only interested in the relative motion, we will just consider the case where $K = 0$, and now the basis is $|i, k; j, k; \pm\rangle$.

The wave function of the exciton in real space can be determined by

$$\psi(I, n; J, l; \pm) = \sum_{ij,k} \langle I, n, \uparrow; J, l, \downarrow | i, k; j, k; \pm \rangle \langle i, k; j, k; \pm | \psi \rangle. \tag{28}$$

The positions of the electron and hole are at site $n$ on the $I$th chain and at site $l$ on the $J$th chain, respectively. $\langle i, k; j, k; \pm|\psi\rangle$ can be obtained by diagonalizing the matrices (19) and (20), and

$$\langle I, n, \uparrow; J, l, \downarrow | i, k; j, k; \pm \rangle = \frac{1}{\sqrt{2}} (\langle c_{In} A_{ik}^\dagger \rangle \langle c_{Jl}^\dagger B_{jk} \rangle \pm \langle c_{In} A_{i-k}^\dagger \rangle \langle c_{Jl}^\dagger B_{j-k} \rangle). \tag{29}$$

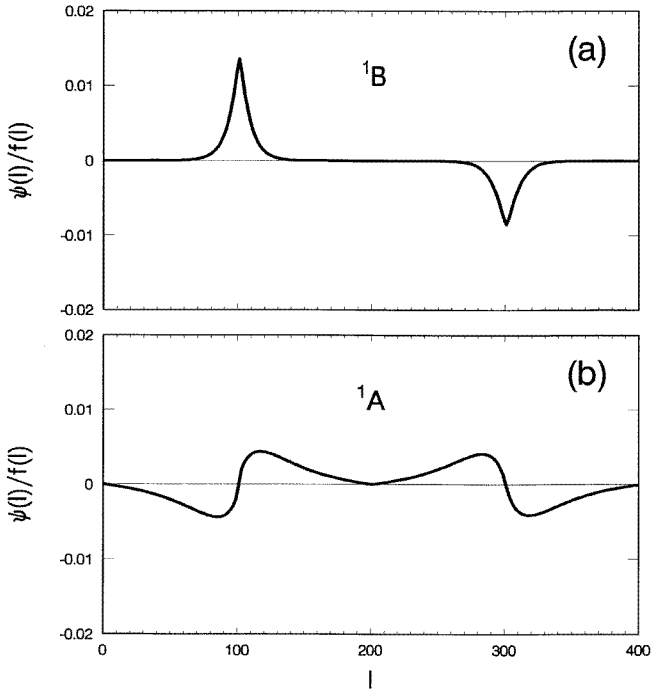


**Figure 1.** Wave functions of the lowest $^1B$- and $^1A$-exciton states for the interchain hopping $t_\perp = 0.15t$ and interchain Coulomb interaction $\tilde{U} = 0.5t$ in the case of parallel ordering between the two chains; (a) is for the $^1B$-state and (b) is for the $^1A$-state.

## 3. Numerical results and discussion

We have carried out numerical calculations to show the properties of excitons in coupled chains. The intrachain parameters are fixed with realistic values, $U = 2t$, $V = t$, and $z = 0.2$. The interchain coupling $t_\perp$ can be estimated according to the results of the LDF calculations for PPV by Vogl and Campbell [27]. In PPV, the total interchain coupling for a pair of monomers $t_{\text{mon}} = 0.64$ eV [28]. Naturally, we set the total coupling for a pair of units in the SSH model $2t_\perp$ to be $t_{\text{mon}}$. Thus $t_\perp$ for PPV ranges from $0.12t$ to $0.15t$. In PPV, the nearest interatom distance on adjacent chains is 2.495 Å [28], while the bond lengths are around 1.4 Å, so the Coulomb interaction strength $\tilde{U} = 0.5t$ is a reasonable estimate for PPV. We will also vary the interchain hopping $t_\perp$ and interchain Coulomb interaction parameter $\tilde{U}$ to make the interchain effects more transparent. The system that we study consists of two chains of $N = 200$. The exciton wave functions in the following figures represent the relative distribution of the hole in different positions when the electron is located at site $n = 101$ on the first chain. The $(200 + i)$th site in figures means the $i$th site of the second chain.

First we study the case of parallel ordering. Figure 1 illustrates the wave functions of the lowest $^1B$- and $^1A$-states with $t_\perp = 0.15t$ and $\tilde{U} = 0.5t$. Since the actual wave function contains rapid staggered oscillation with a period of $4a$, we have plotted $\psi(I = 1, n = 101; J, l; \pm)/f(l)$ with $f(l) = \sqrt{2}\cos[(\pi/2)(l + \frac{1}{2})]$ for the odd number $l$ [18]. We give in tables 1 and 2 the exciton energy $E_{\text{ex}}$ and the probability $P$ that the hole is in the second chain for several groups of $t_\perp$ and $\tilde{U}$. From these tables, we can see that

**Table 1.** The interchain parameters ($t_\perp$ and $\tilde{U}$) and resulting exciton properties ($E_{ex}$ and $P$) of the lowest $^1B$ states for the case of parallel ordering between the two chains.

| $t_\perp,\ \tilde{U}(t)$ | 0.03, 0.5 | 0.03, 1.0 | 0.09, 0.5 | 0.09, 1.0 | 0.15, 0.5 | 0.15, 1.0 |
|---|---|---|---|---|---|---|
| $E_{ex}(t)$ | 1.095 | 1.057 | 1.010 | 0.941 | 0.902 | 0.821 |
| $P$ | 0.062 | 0.300 | 0.241 | 0.428 | 0.330 | 0.457 |

**Table 2.** The interchain parameters ($t_\perp$ and $\tilde{U}$) and resulting exciton properties ($E_{ex}$ and $P$) of the lowest $^1A$-states for the case of parallel ordering between the two chains.

| $t_\perp,\ \tilde{U}(t)$ | 0.03, 0.5 | 0.03, 1.0 | 0.09, 0.5 | 0.09, 1.0 | 0.15, 0.5 | 0.15, 1.0 |
|---|---|---|---|---|---|---|
| $E_{ex}(t)$ | 1.345 | 1.331 | 1.229 | 1.211 | 1.109 | 1.091 |
| $P$ | 0.335 | 0.463 | 0.446 | 0.488 | 0.468 | 0.493 |

the hole has more probability of staying in the second chain for both $B$- and $A$-states as the interchain hopping $t_\perp$ and interchain Coulomb interaction $\tilde{U}$ increase. Since the energies of the $A$-states are close to the continuum band and the wave functions extend over almost the whole system, the amplitude of the wave function in the second chain is comparable to that of the first chain. The energies of $B$-states sit, however, deep in the gap, so the amplitude of the wave function in the second chain is smaller and depends more sensitively on the interchain couplings than in the case of $A$-states. The triplet has similar features to the singlet.

**Table 3.** The interchain parameters ($t_\perp$ and $\tilde{U}$) and resulting exciton properties ($E_{ex}$, $P$, and $d$) of the lowest $^1B$-states for the case of anti-parallel ordering.

| $t_\perp,\ \tilde{U}(t)$ | 0.03, 0.5 | 0.03, 1.0 | 0.09, 0.5 | 0.09, 1.0 | 0.15, 0.5 | 0.15, 1.0 |
|---|---|---|---|---|---|---|
| $E_{ex}(t)$ | 1.110 | 1.096 | 1.110 | 1.095 | 1.108 | 1.093 |
| $P$ | 0.005 | 0.007 | 0.045 | 0.059 | 0.111 | 0.139 |
| $d(a)$ | 7 | 7 | 7 | 7 | 7 | 7 |

**Table 4.** The interchain parameters ($t_\perp$ and $\tilde{U}$) and resulting exciton properties ($E_{ex}$, $P$, and $d$) of the lowest $^1A$-states for the case of anti-parallel ordering.

| $t_\perp,\ \tilde{U}(t)$ | 0.03, 0.5 | 0.03, 1.0 | 0.09, 0.5 | 0.09, 1.0 | 0.15, 0.5 | 0.15, 1.0 |
|---|---|---|---|---|---|---|
| $E_{ex}(t)$ | 1.345 | 1.194 | 1.328 | 1.188 | 1.308 | 1.178 |
| $P$ | 0.913 | 0.987 | 0.701 | 0.903 | 0.609 | 0.798 |
| $d(a)$ | 9 | 7 | 9 | 7 | 7 | 5 |

Now we divert our attention to the case of anti-parallel ordering, which is more likely to be realized in practical polymers [29]. Additionally, the features of the exciton in this case are more interesting. We describe the lowest $^1B$- and $^1A$-states for $t_\perp = 0.15t$ and $\tilde{U} = 0.5t$ in figure 2. We have plotted $\psi(I = 1, n = 101; J, l; \pm)/f(l)$ for $l$ an odd number when $J = 1$ but for $l$ an even number when $J = 2$. The exciton energy $E_{ex}$, the probability $P$ that the hole stays in the second chain, and the separation $d$ between positions of maxima

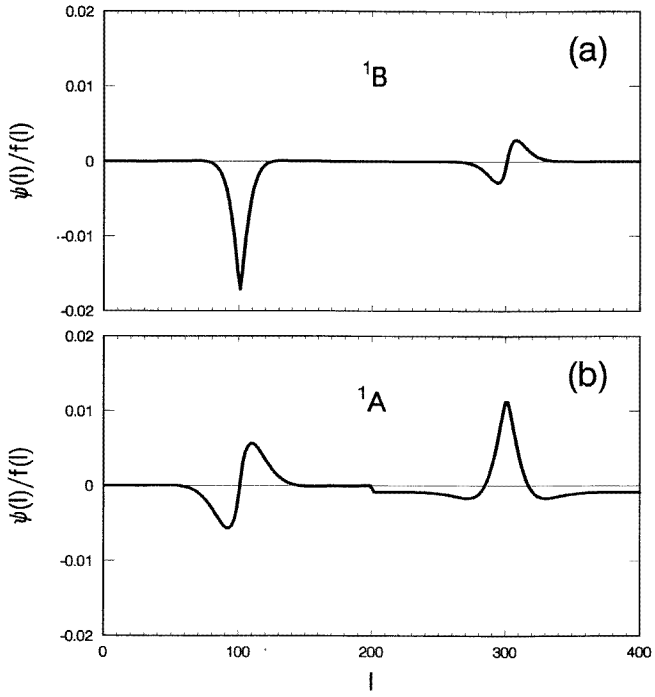


**Figure 2.** Wave functions of the lowest $^1B$- and $^1A$-exciton states for $t_\perp = 0.15t$ and $\tilde{U} = 0.5t$ in the case of anti-parallel ordering; (a) is for the $^1B$-state and (b) is for the $^1A$-state.

of the wave-function amplitude in the two chains are listed in tables 3 and 4 for several groups of the interchain parameters. It is shown that a larger $\tilde{U}$ leads to a greater chance of finding the hole in the second chain. However, the dependence of the probability $P$ on the interchain coupling $t_\perp$ is not so simple as in the case of parallel ordering. For the $^1B$-state, $P$ becomes larger when $t_\perp$ increases, while for the $^1A$-state, in contradiction with intuition, $P$ decreases as $t_\perp$ increases. Unlike for parallel ordering, where the profiles of the wave functions in the two chains are alike and the maxima of the wave-function amplitude in the two chains sit at the same position, in the case of anti-parallel ordering, the wave functions in the two chains are very different from each other. For $^1B$-states, when the hole approaches the position of electron $n = 101$ on the first chain, the wave function reaches the maximum; but on the second chain, the wave function goes to zero when the hole is nearest to the electron. While, for $^1A$-states, when the hole and electron overlap on the first chain, the wave function vanishes; but when the hole is on the second chain, the wave function reaches the maximum as the hole approaches the position of the electron. The positions with the largest wave-function amplitudes in the two chains have a separation $\sim 5a$–$9a$ for both $B$- and $A$-states. The interchain Coulomb interaction can reduce this separation to a certain extent. This big difference between the two ordering cases is understandable. From equations (9) and (13), we can see that, in the case of parallel ordering, there is no mixing between valence and conduction bands of different chains and the system is more like a two-independent-chain system; in the case of anti-parallel ordering, however, the valence and conduction band states of these two chains are mixed together and the two chains are really *coupled*.

For PPV, there are two kinds of ordering between adjacent chains, namely, in-phase and out-of-phase ordering [30–32]. When the practical structure of PPV is mapped into the simplified SSH model as stated before, each type of ordering is neither parallel nor anti-parallel and the wave function of the exciton in PPV should therefore be composed from those for parallel and anti-parallel ordering. For the $^1B$-state, from figures 1(a) and 2(a), the maximum of the composed wave function in the first chain should sit at the position of the electron, since the profiles of the wave functions for parallel and anti-parallel ordering are the same; while, in the second chain, the position of maximum for the composed wave function must be situated between the site facing the electron and the site where the maximum in the second chain occurs for anti-parallel ordering. For the $^1A$-state, from figures 1(b) and 2(b), the composed wave function in the first chain will vanish at the position of the electron, and reach the maximum at the site which lies between the position of the electron and that of the maximum for parallel ordering. The shape of the composed wave function, which shows that the position of the maximum in the second chain deviates from the location of the electron in the first chain, implies that if the interchain exciton is produced, the electron and hole tend to be separated by several lattice constants. This is similar to the concept of the 'spatially indirect exciton' proposed by Yan and co-workers to interpret the PA spectrum in PPV [6, 7]. We emphasize that it is the exchange effect which prevents the electron and hole in different chains from approaching each other in the presence of the interchain electron–electron interaction, and previous treatments of the interchain Coulomb interaction, in which only the electrostatic energy is included [33], cannot predict this feature. Another interesting property is that, for the $A$-state, the interchain exciton is even more likely to be created than the intrachain exciton. Recently, it was documented that 80%–90% of photoexcitations in PPV are interchain excitations [6], since in practical materials, defects, interfaces, and thermal fluctuations can lead to charge transfer and mixing between the $A$- and $B$-states, and the $A$-states with large possibilities of interchain excitons seem to make contributions to the great number of interchain excitations in PPV. Obviously, these interchain excitations are also important to the PC, which is thought of as an interchain process in PPV.

In summary, we have studied the excitons in two coupled polymer chains. The wave functions of the lowest $A$- and $B$-states for both parallel and anti-parallel ordering have been illustrated. We have shown the pronounced difference between the properties of excitons for these two kinds of ordering. For the realistic PPV, whose properties should be combinations of those for each ordering type, the electron and hole tend to be separated by several lattice constants when they are not in the same chain, and in the $A$-state the probability that the electron and hole are in different chains is even larger than the probability that they are in the same chain. These features are helpful to clarify the controversies involved in interpreting experiments on luminescent polymers like PPV.

## Acknowledgments

This work was partly supported by the National Natural Science Foundation and the Advanced Materials Committee of China. Part of the numerical calculation of the present work was carried out when ZGY was visiting Tianjin, People's Republic of China, in the vacation. He thanks Yi Hou for her hospitality and help during his stay there. One of the authors (MWW) was supported by the US Office of Naval Research (Contract No N66001-95-M-3472) and the US Army Research Office (Contract No DAAH04-94-G-0413).

## Appendix

In this appendix, we demonstrate how to calculate $\langle c^{\dagger}_{Il} A_{ik_c}\rangle$, $\langle B^{\dagger}_{jk_v} c_{Il}\rangle$, and $\langle c^{\dagger}_{Jl'} c_{Il}\rangle$. It is noted that

$$\langle c_{Il} A^{\dagger}_{ik_c}\rangle = \langle Il|A^{\dagger}_{ik_c}|0\rangle \tag{A1}$$

$$\langle B^{\dagger}_{jk_v} c_{Il}\rangle = \langle Il|B^{\dagger}_{ik_v}|0\rangle \tag{A2}$$

and

$$\langle c^{\dagger}_{Jl'} c_{Il}\rangle = \sum_{ik_v} \langle 0|B_{ik_v}|Jl'\rangle\langle Il|B^{\dagger}_{ik_v}|0\rangle. \tag{A3}$$

Since from equations (3) and (4), we have

$$\begin{pmatrix} \langle 2n|\alpha^{\dagger}_{jk}|0\rangle & \langle 2n+1|\alpha^{\dagger}_{jk}|0\rangle \\ \langle 2n|\beta^{\dagger}_{jk}|0\rangle & \langle 2n+1|\beta^{\dagger}_{jk}|0\rangle \end{pmatrix} = \frac{1}{\sqrt{N}} \mathrm{e}^{\mathrm{i}k2n} \begin{pmatrix} \exp(-\mathrm{i}\theta_{jk}) & -\exp(\mathrm{i}\theta_{jk}+\mathrm{i}k) \\ \mathrm{i}\exp(-\mathrm{i}\theta_{jk}) & \mathrm{i}\exp(\mathrm{i}\theta_{jk}+\mathrm{i}k) \end{pmatrix} \tag{A4}$$

with

$$\cos\theta_{jk} = \frac{1}{\sqrt{2}}\left(1+\frac{\epsilon_k}{E_k}\right)^{1/2} \tag{A5}$$

$$\sin\theta_{jk} = \frac{z_j \sin k}{|z_j \sin k|}\frac{1}{\sqrt{2}}\left(1-\frac{\epsilon_k}{E_k}\right)^{1/2} \tag{A6}$$

where $\epsilon_k = 2t\cos k$, then combining equation (A4) with the transformation matrix $\mathbf{O}$, we can obtain $\langle c^{\dagger}_{Il} A_{ik_c}\rangle$, $\langle B^{\dagger}_{jk_v} c_{Il}\rangle$, and $\langle c^{\dagger}_{Jl'} c_{Il}\rangle$.

## References


[1] Chemla D S and Zyss J 1987 *Nonlinear Optical Properties of Organic Molecules and Crystals* vol 2 (New York: Academic)
[2] Burroughes J H, Bradley D D C, Brown A R, Marks R N, MacKay K, Friend R H, Burn P L and Holmes A B 1990 *Nature* **347** 539
[3] Frankevich E L, Lymarev A A, Sokolik I, Karasz F E, Blumstengel S, Baughman R H and Hörhold H H 1992 *Phys. Rev.* B **46** 9320
[4] Lee C H, Yu G, Moses D and Heeger A J 1994 *Phys. Rev.* B **49** 2396
[5] Leng J M, Jeglinski S, Wei X, Beener R E and Vardeny Z V 1994 *Phys. Rev. Lett.* **72** 156
[6] Yan M, Rothberg L J, Papadimitrakopoulos F, Galvin M E and Miller T M 1994 *Phys. Rev. Lett.* **72** 1104; 1994 *Phys. Rev. Lett.* **73** 744
[7] Hsu J W P, Yan M, Jedju T M and Rothberg L J 1994 *Phys. Rev.* B **49** 712
[8] Chandross M, Mazumdar S, Jeglinski S, Wei X, Vardeny Z V, Kwock E W and Miller T M 1994 *Phys. Rev.* B **50** 14 702
[9] Gomes da Costa P and Conwell E M 1993 *Phys. Rev.* B **48** 1993
[10] Yu Z G, Fu R T, Wu C Q, Sun X and Nasu K 1995 *Phys. Rev.* B **52** 4849
[11] Guo F, Chandross M and Mazumdar S 1995 *Phys. Rev. Lett.* **74** 2086
[12] Yan M, Rothberg L J, Kwock E W and Miller T M 1995 *Phys. Rev. Lett.* **75** 1992
[13] Pichler K, Halliday D A, Bradley D D C, Burn P L, Friend R H and Holmes A B 1993 *J. Phys.: Condens. Matter* **5** 7155
[14] Halliday D A, Burn P L, Bradley D D C, Friend R H, Gelsen O, Holmes A B, Kraft A, Martens J H F and Pichler K 1993 *Adv. Mater.* **5** 40
[15] Suhai S 1984 *Phys. Rev.* B **29** 4570
[16] Hayashi H and Nasu K 1985 *Phys. Rev.* B **32** 5295
[17] Tanaka H, Inoue M and Hanamura E 1987 *Solid State Commun.* **63** 103
[18] Abe S, Yu J and Su W P 1992 *Phys. Rev.* B **45** 8264
[19] Nakajima S, Toyozawa Y and Abe R 1980 *The Physics of Elementary Excitations* (Berlin: Springer)
[20] Baeriswyl D and Maki K 1983 *Phys. Rev.* B **24** 2068

[21] Heeger A J, Kivelson S, Schrieffer J R and Su W P 1988 *Rev. Mod. Phys.* **60** 781
[22] Peierls R E 1955 *Quantum Theory of Solids* (Oxford: Clarendon)
[23] Soos Z G, Etemad S, Galvão D S and Ramasesha S 1992 *Chem. Phys. Lett.* **194** 341
Soos Z G, Ramasesha S, Galvão D S and Etemad S 1993 *Phys. Rev.* B **47** 1742
[24] Farchioni R, Grosso G and Pastori Parravicini G 1996 *Phys. Rev.* B **53** 4294
[25] Shuai Z, Pati S K, Su W P, Brédas J L and Ramasesha S 1996 unpublished
[26] Beljonne D, Shuai Z, Friend R H and Brédas J L 1995 *J. Chem. Phys.* **102** 2042
[27] Vogl P and Campbell D K 1990 *Phys. Rev.* B **41** 12 797
[28] Mizes H A and Conwell E M 1995 *Synth. Met.* **68** 145
[29] Fincher C R, Chen C E, Heeger A J, MacDiarmid A G and Hastings J B 1982 *Phys. Rev. Lett.* **48** 100
[30] Chen D, Winokur M J, Masse M A and Karasz F K 1990 *Phys. Rev.* B **41** 6759
[31] Zhang C, Braun D and Heeger A J 1993 *J. Appl. Phys.* **73** 5177
[32] Bradley D D C, Friend R H, Hartmann T, Marseglia E A, Sokolowski M M and Townsend P D 1987 *Synth. Met.* **17** 473
[33] Mizes H A and Conwell E M 1994 *Phys. Rev.* B **50** 11 243